

Tribocorrosion on Mars

Javier Martin-Torres (✉ javier.martin-torres@abdn.ac.uk)

University of Aberdeen

Maria-Paz Zorzano

University of Aberdeen

Erik Nyberg

Luleå University of Technology <https://orcid.org/0000-0002-0851-8475>

Abhilash Vakkada Ramachandran

Luleå University of Technology <https://orcid.org/0000-0003-0499-6370>

Anshuman Bhardwaj

Luleå University of Technology

Article

Keywords:

Posted Date: June 23rd, 2020

DOI: <https://doi.org/10.21203/rs.3.rs-36280/v1>

License:   This work is licensed under a Creative Commons Attribution 4.0 International License.

[Read Full License](#)

1 **TRIBOCORROSION ON MARS**

2

3 **Javier Martin-Torres^{1,2,3}, María-Paz Zorzano^{4,1,3}, Erik Nyberg³, Abhilash Vakkada-**
4 **Ramachandran³, Anshuman Bhardwaj³**

5 ¹School of Geosciences, University of Aberdeen, U.K.

6 ²Instituto Andaluz de Ciencias de la Tierra (CSIC-UGR), Armilla, Granada, Spain

7 ³ Department of Computer Science, Electrical and Space Engineering, Luleå University of
8 Technology, Luleå, Sweden

9

10 ⁴ Centro de Astrobiología (CSIC-INTA), Torrejón de Ardoz, Madrid, Spain

11

12

13 **ABSTRACT**

14 Tribocorrosion is a degradation phenomenon of material surfaces subjected to the combined
15 action of mechanical loading and corrosion attack caused by the environment. Although
16 corrosive chemical species such as materials like chloride atoms, chlorides and perchlorates
17 have been detected on the Martian surface, there is a lack of studies of its impact on materials
18 for landed spacecraft and structures that will support surface operations on Mars. Here we
19 present a series of experiments on the stainless-steel material of the ExoMars 2020 Rosalind
20 Franklin rover wheels. We show how tribocorrosion induced by brines accelerate wear on the
21 materials of the wheels. Our results do not compromise the nominal ExoMars mission but have
22 implications for future long-term surface operations in support of future human exploration or
23 extended robotic missions on Mars.

24

25 **Introduction**

26 Tribocorrosion is a surface damage phenomenon resulting from the synergistic action of
27 mechanical wear and (electro)chemical reactions. It can imply corrosion accelerated by wear,

28 or wear accelerated by chemical reactions¹. It was discovered in 1875 by Thomas Edison, who
29 observed a variation in the coefficient of friction between metal and chalk moistened with
30 electrolyte solutions², and today is an important engineering topic, defined by ISO³ and
31 ASTM⁴, and a cause for concern to any engineer employing passive metal components in
32 corrosive environments⁵. If adequately controlled, tribocorrosion can be beneficial, such as in
33 machinery lubricants where it is used as a means of avoiding seizure by promoting wear in a
34 sacrificial mode⁶.

35

36 The surface of Mars is rich in corrosive chemical species. Martian regolith contains chloride
37 in abundance⁷ which forms various chlorides and perchlorate salts with high solubilities and
38 low eutectic temperatures^{8,9}. Detection of 0.4-0.6% perchlorate by mass in Martian high
39 latitudes and further revelation of soluble chemistry of Martian soil at the Phoenix Lander site¹⁰
40 were encouraging results prompting researchers to focus on perchlorate-based brine research.
41 Other remaining anions and cations, as detected by the Wet Chemistry Laboratory on the
42 Phoenix Mars Lander were chloride, bicarbonate, and sulphate and Mg²⁺, Na⁺, K⁺, and Ca²⁺,
43 respectively¹⁰. Subsequently, the reanalysis of the Viking results also suggested the plausible
44 presence of perchlorate and organics at midlatitudes on Mars¹¹. Evidence for sodium
45 perchlorate (NaClO₄), magnesium perchlorate (Mg(ClO₄)₂) and calcium perchlorate
46 (Ca(ClO₄)₂) has also been provided at equatorial latitudes by the Sample Analysis at Mars
47 instrument on the Mars Science Laboratory (MSL)¹². Another study¹³ provides evidence of
48 Martian perchlorate, chlorate, and nitrate in the Martian meteorite EETA79001 with
49 sufficiently high concentrations. These results indicate the possibility that perchlorates might
50 be abundantly present within Martian regolith at all latitudes. A variety of pathways have been
51 proposed for the perchlorate synthesis on Mars. These pathways may involve photochemical
52 reactions¹⁴, electrostatic discharge¹⁵, and oxidation-reduction reactions¹⁶. Perchlorates and

53 chloride salts in the Martian regolith are extensively investigated because they can absorb
54 water from the atmosphere forming hydrates¹⁷, by absorption, and then liquid brines, through
55 deliquescence^{18,19}. In addition to perchlorates, chlorides such as FeCl₃, CaCl₂, and MgCl₂ can
56 also act as strong freezing point depressants. FeCl₃ and CaCl₂ are the strongest freezing point
57 depressants with eutectic temperatures as low as approximately 218 K, followed by MgCl₂,
58 NaCl, and KCl at about 238 K, 252 K, and 262 K, respectively⁹.

59 Perchlorates (ClO₄⁻) have been found planet-wide on Mars¹⁰. Studies show that the
60 perchlorate salts which contains ClO₄⁻ anion can hold the water in brine state even when the
61 temperature reaches 203 K. Other chloride (Cl⁻) salts have been detected such as magnesium
62 chloride (MgCl₂) and calcium chloride (CaCl₂)²⁰, along with sulphate salts such as iron
63 sulphate²¹, which has deliquescent properties.

64

65 A recent work²² has derived the current chemical weathering rates on Mars, based on the
66 oxidation of iron in stony meteorites investigated by the Mars Exploration Rover Opportunity
67 at Meridiani Planum. The authors concluded that the chemical weathering rates derived are ~1
68 to 4 orders of magnitude slower than that of similar meteorites found in Antarctica where the
69 slowest rates are observed on Earth, suggesting aridity of Mars to be even more significant than
70 expected during the last 50 Myr. The authors extrapolated their results to the impact of
71 weathering in the wheels of the NASA Curiosity rover, pointing that “Martin-Torres and co-
72 workers¹⁸ worry that the corrosive effects of chlorine brine might pose a challenge to
73 spacecraft. The extremely slow weathering of meteorites, which contain metallic iron as a
74 phase very sensitive towards chemical alteration, suggests that this is not a threat over the
75 lifetime of a spacecraft, however. The Opportunity rover is testament to that, showing no signs
76 of chemical weathering or corrosion after more than 12 years of operating on Mars (April
77 2016).”

78

79 The argument used by Schroeder et al. to justify the absence of corrosion on mechanical parts
80 on Mars actually supports the hypothesis that environmental conditions have an impact on the
81 fate of the rover wheels. The wheels of Opportunity and Curiosity were similar in terms of
82 composition and effective ground pressure supported (see Materials and Methods). The fact
83 that Opportunity showed no signs of chemical weathering or corrosion after more than 14 earth
84 years of operation on Mars (from 2004 until the middle of 2018), while Curiosity rover faced
85 extreme corrosion and related punctures and tears just months after landing on Mars, maybe
86 an indication of the impact of the local environment on wheels weathering. Actually, the details
87 of this wear and tear on the wheels of Curiosity Rover are missing from Schröder et al. 22.

88 Corrosion of the surface of a metal is the degradation that results from its chemical interaction
89 with the environment. On Mars, any metal facing the sky, as the observable side of a meteorite,
90 would only be exposed to the air and thus only ambient oxygen would produce this damage.
91 This is the case analysed by Schroeder et al., which considers only the chemical weathering
92 rates of metals exposed to the Martian atmosphere. However, in the case of metals in contact
93 with the regolith, as it is the case of the metals used in the wheels of the rovers operating on
94 Mars, these materials may be eventually directly exposed to Cl and brines, which are formed
95 naturally under Martian conditions at the interface of the regolith and the atmosphere¹⁷⁻¹⁹.
96 These two processes are very different, as in the case of the wheels, in addition to the exposure
97 to a liquid phase, there is the additional damage of mechanical wearing. It is known, that metal
98 can be protected from corrosion by covering it with a coating, such as an anodised treatment,
99 however as soon as this protective layer is scratched or worn-out the inner material is directly
100 exposed to corrosion. The Curiosity's wheel is made from a single piece of machined
101 aluminium alloy AA7075-T7351. The main rim is 1.9 cm thick (0.75-inches)²³. Martin-Torres
102 et al. 18 hypothesised that the daily contact of the wheels with the corrosive perchlorate

103 solutions during every night may have weakened the scratched surface of the anodised
104 aluminium, making it more susceptible to damage against sharp rocks. Although the large
105 cracks observed in the wheels of Curiosity are likely caused by mechanical damage, an image
106 taken by the ChemCam remote microscopic-imager on sol 502 the vertical wall of the T-print
107 of the wheels, showed a pattern of distributed sub-millimetre sized blisters that cannot be
108 attributed to rock scratching and resembled aluminium alloy pitting corrosion²⁴. Unfortunately,
109 the Spirit and Opportunity rovers did not have an equivalent camera to analyse the wheels with
110 submillimetre precision, so we cannot state whether this damage existed or not.

111 Previous preliminary experiments, designed to look at the interaction between aerospace
112 aluminium alloy (AA7075-T73) and the gases present in the Mars atmosphere, at 20°C and a
113 pressure of 700 Pa with only 0.13% of oxygen, showed that there is an interaction between the
114 small amount of oxygen present in the Mars gas and the alloy, when there is a scratch that
115 removes the protective aluminium oxide film²⁵. The anodising process that is applied to
116 aluminium alloy increases the thickness of the natural oxide layer on the aluminium wheels,
117 but the abrasion can wear out the external protecting layer and expose the bare aluminium
118 metal to corrosion. The purpose of this work is to evaluate the role of direct contact with liquid
119 brines and the additional damage caused by mechanical friction.

120

121 **Results**

122 Here we present laboratory studies that show the impact of tribocorrosion (the combination of
123 mechanical and corrosion wearing) on materials in contact with naturally formed brines under
124 current environmental conditions on Mars. Although tribocorrosion is a well-known
125 phenomenon since nearly 150 years ago, there is a lack of analysis of its impact on materials
126 for landed spacecraft and structures that will support surface operations on Mars. Mechanical
127 parts, like the wheels of the rovers operating on Mars, in contact with corrosive brines on the

128 surface, could be affected by the combination of chemical corrosion and mechanical loading.
129 Nevertheless, to our knowledge, not a single research on tribocorrosion research on Mars has
130 ever been published. This, in spite of the fact that corrosive materials have been found on the
131 surface of Mars.

132

133 The European Space Agency ExoMars 2022 Rosalind Franklin rover will have a nominal
134 lifetime of 218 sols (around 7 Earth months). Its mass is 310 kg, with an instrument payload
135 of 26 kg (excluding payload servicing equipment such as the drill and sample processing
136 mechanisms). The rover's kinematic configuration is based on a six-wheel, triple-bogie concept
137 with locomotion formula $6 \cdot 6 \cdot 6 + 6$, denoting six supporting wheels, six driven wheels, and
138 six steered wheels, plus six articulated (deployment) knee drives. This system enables the rover
139 to passively adapt to rough terrains, providing inherent platform stability without the need for
140 a central differential²⁶. The wheels are made of Sandvik stainless spring steel (11R51).

141

142 Here we have performed laboratory studies on how the material (stainless spring steel) used in
143 ExoMars 2022 Rosalind Franklin rover wheels is affected first by corrosion and then by
144 tribocorrosion under environmental conditions on Mars. We suggest that similar studies should
145 be applied to other materials used for wheels and structures in contact with the Martian regolith.

146

147

148

149 **Brine corrosion under Martian conditions**

150 For the study of corrosion, we have tested samples of the Sandvik 11R51 stainless steel, used
151 in the ExoMars 2022 Rosalind Franklin rover wheels, and two other control materials: stainless
152 steel SS4301, and regular steel S235. Sandvik 11R51 is an austenitic stainless steel with

153 excellent spring properties with higher corrosion resistance (due to the addition of
 154 molybdenum), mechanical strength, tensile strength and tempering effect, and fatigue and
 155 relaxation properties that other stainless steels. Every material was exposed to two sets of salt
 156 environments inside the SpaceQ chamber at Martian conditions²⁷, and three control tests with
 157 salt (see Table 1) under ambient laboratory conditions (20 C and 1010 mbar).
 158

Case		Salt Environments
#1	SpaceQ martian conditions	1.5g NaClO ₄ (+water spontaneously absorbed from the atmosphere)
#2	SpaceQ martian conditions	1.5g MMS soil + 0.15 g NaClO ₄ salt (+water spontaneously absorbed from the atmosphere)
Control #1	Laboratory conditions	NaClO ₄ (1.5g salt + 1g water) Brine immersion
Control #2	Laboratory conditions	1.5g MMS soil + 0.15 g NaClO ₄ salt
Control #3	Laboratory conditions	Indoors (exposed to the air at ambient lab conditions)

159 **Table 1.** Environmental conditions of the experiments performed with 11R51, SS4301 and
 160 S235

161

162 Cases #1 and #2 were exposed 5 hours to the Martian environment within the SpaceQ chamber,
163 and to the simulated Martian water cycle described in Methods and Materials. The set of
164 control samples #1, #2 and #3 were left on the bench at laboratory conditions during the same
165 time, and the control sample #1 was immersed in a brine of NaClO₄ (1.5g salt + 1g water) to
166 observe the reactivity of the material within the liquid already formed. After the
167 experiments, the samples were packed in an airtight bag and studied using a scanning electron
168 microscope (SEM) along with elemental detection via Electron Dispersive X-ray Spectroscopy
169 (EDS) to determine the effects of corrosion.

170 The overview of the optical inspection by digital microscopy is shown in Table 2. We found
171 no corrosion on either of the stainless-steel samples (11R51 or SS4301). On the contrary, the
172 regular steel sample (Reg S235) presented visible signs of corrosion, both in Case #1
173 (simulated Mars environment and immersed in the brine that is formed spontaneously by
174 absorption of the moisture in the air), and in Case #2 (simulated Mars environment and
175 immersed in soil + salt), whereas the same immersion under ambient atmosphere produced less
176 corrosion (Control #2). It is worth pointing out that these brines are formed spontaneously and
177 are stable at Martian surface conditions.

178

179 In order to identify spectrally the corrosion in S235 under Case #1 we performed the analysis
180 with the SEM-EDS as seen in Figure 7 (a–c). The digital microscope image in (a) shows clear
181 visible signs of corrosion. A region that included corroded and non-corroded steel was selected
182 for high magnification studies (green box). In (b), four regions along a vertical line were
183 selected for EDS analysis. The EDS spectra in (c) show that regions related to spectrum 3 and
184 4 are enriched in carbon (C at 0.27 keV), oxygen (O at 0.52 keV) and sodium (Na at 1.04 keV)
185 compared to the reference regions in spectrum 1 and 2. These results are evidence of oxidation
186 of the regular steel by the sodium perchlorate brine. Interestingly carbon and oxygen, from the

187 Martian atmosphere and the water in the brine and air, have also been fixed with different
188 efficiencies from site 1 to 4, depending on the redox state of the material after the corrosion.
189 Actually, it is worth to remark that upon exposure to two different environments the regular
190 steel was more severely corroded under Martian conditions (Cases #1 and #2) that under
191 ambient conditions (see for comparison Case #2 vs Control# 2 in Table 2), so the corrosion of
192 regular steel S235 is amplified under Martian conditions. The brines were effectively formed
193 under Martian conditions because of the high relative humidity conditions, whereas at ambient
194 conditions in the laboratory the relative humidity was moderated.

195

196

197

198

199

200

201

202

203

204

205

206

207

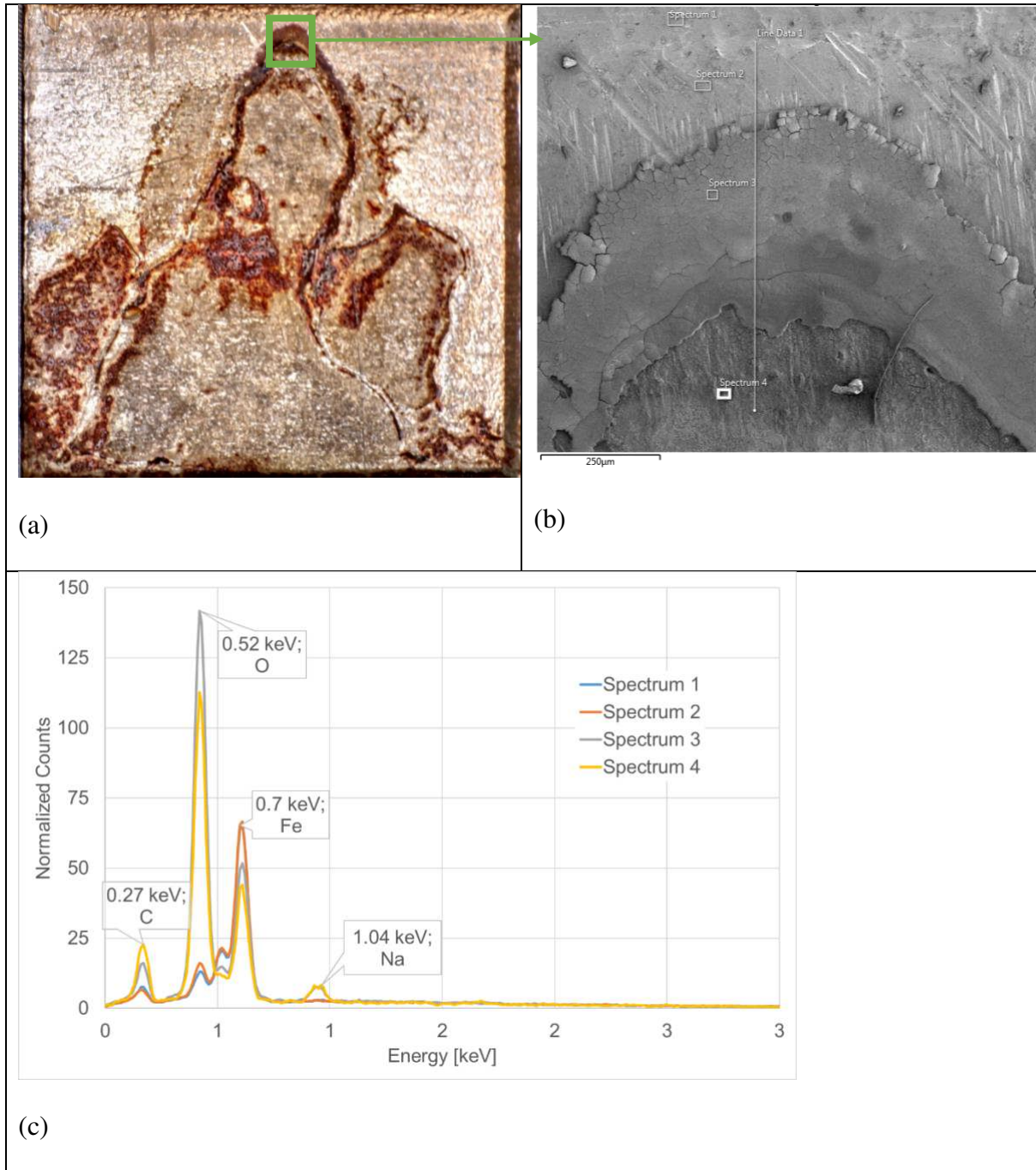
208

209

210

Condition	Sandvik 11R51	SS4301	Reg S235
Case #1 (SpaceQ Brine)	 No corrosion	 No corrosion	 Severe Corrosion
Case # 2 (SpaceQ Soil+Salt)	 No corrosion	 No corrosion	 Severe Corrosion
Control 1 (Ambient Brine)	 No corrosion	 No corrosion	N/A Insufficient samples. Severe corrosion expected.
Control 2 (Ambient Soil+Salt)	 No corrosion	 No corrosion	 Corrosion
Control 3 (Ambient)	 No corrosion	 No corrosion	 No corrosion

211 **Table 2.** Optical inspection of the experiments.



213

214 **Figure 1:** (a) Microscope image of 10x10 mm Regular Steel sample. (b) High magnification

215 SEM image showing location of EDS analyzed regions. (c) results of EDS analysis confirming

216 corrosion by detection of Na and O in Spectrum 3 and 4.

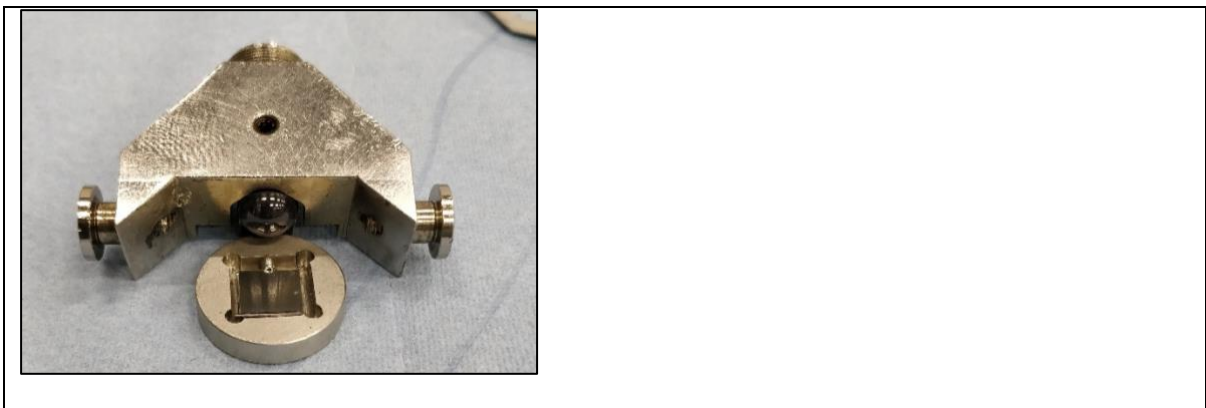
217

218 Discussion

219 Tribocorrosion under martian conditions

220 As shown in Table 2 the material used in the ExoMars wheels (stainless spring steel Sandvik
221 11R51) showed no corrosion. We have conducted a tribological experiment to evaluate if it is
222 feasible to corrode (oxidize) stainless steel when subjected to wear while exposed to a liquid
223 brine of the type that can be formed under Martian conditions. The experiment was conducted
224 by rubbing for 90 minutes a 10 mm ceramic (Si_3N_4) ball against the material, while the plate
225 was immersed in either brine or water (see Fig. 2 with the setup). This is a standard procedure
226 for testing tribocorrosion.

227



228 **Figure 2.** Setup of tribological experiment showing ceramic ball and stainless-steel plate in
229 their respective sample holders.

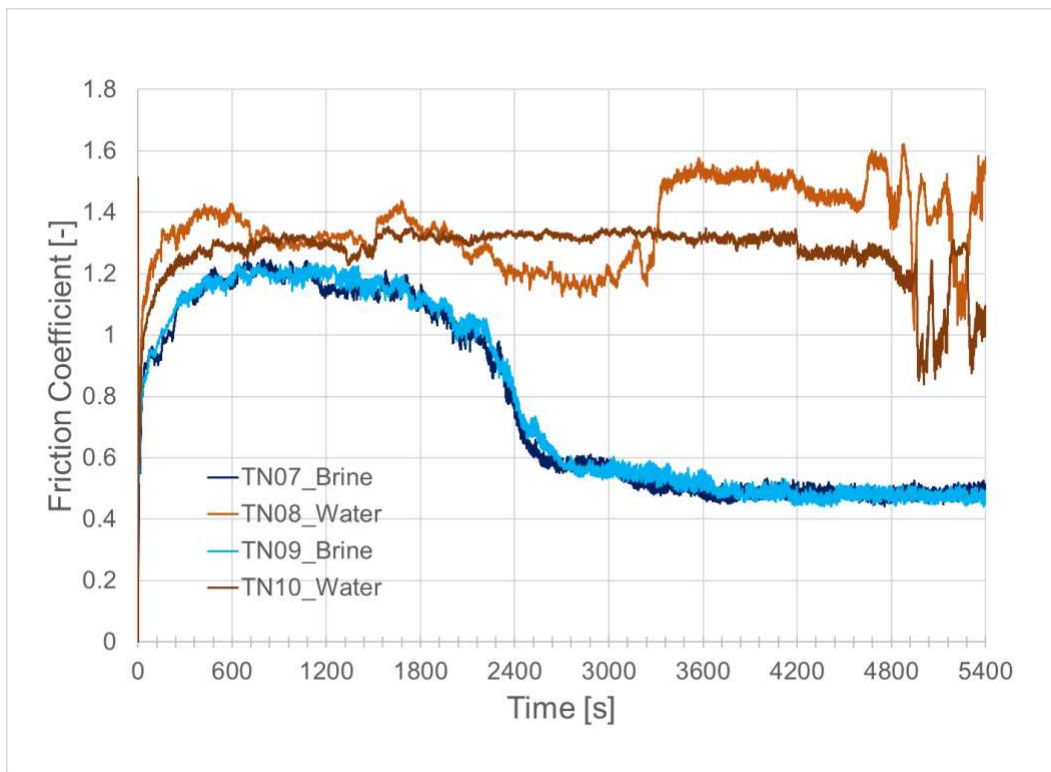
230

231 For the analysis we included (see Methods and Materials): (i) measurements of friction during
232 rubbing; (ii) wear volume by 3D optical profilometer; (iii) optical inspection with digital
233 microscope; and (iv) scanning electron microscopy and electron dispersive X-ray spectroscopy
234 (SEM-EDS) for detailed surface analysis including chemical (elemental) analysis.

235 Figure 3 shows the friction data and shows a clear difference between testing in water or

236 brine. The friction coefficient is initially increasing to values above 1, but for the wear test in

237 brine the friction drops significantly after 30 min (1800 s). The drop-in friction could be
238 explained by the chemical reactions that reduce the surface integrity and thereby lowers
239 friction. In tribology, this is known as sacrificial wear and is commonly employed in the anti-
240 seizure chemical additives known as extreme pressure agents (EP). Chlorine containing EP
241 agents have historically been used, but are not recommended as they may cause corrosion²⁸.
242



243
244 **Figure 3.** Friction data indicates transition to corrosive wear around Time=1800 s when
245 immersed in brine.

246
247 Table 3 shows that the worn volume is significantly increased (>45%) when the test is
248 performed in brine instead of water. TN10 has the lowest worn volume of all samples,
249 indicating that brines have >45% worn volume in these experiments.

	Worn Volume [μm^3]	Max depth [μm]	Projected area [mm^2]	Worn Volume per cycle [μm^3]
TN07 Brine	80 466 771	41.2	3.16	1490
TN08 Water	54 217 302	38.4	3.59	1004
TN09 Brine	78 590 249	40.5	3.19	1455
TN10 Water	26 081 611	19.6	3.53	483

251 **Table 3.** Wear data.

252

253 The wear marks are shown in 4 after washing the samples in two steps in heptane and ethanol
 254 in ultrasonic bath. The samples tested in water show a visual appearance that could be
 255 interpreted as corrosion, while the samples tested in brine are brighter in appearance except for
 256 along the edges. The repeatability is good. Figure 5 are an overview of the reference samples
 257 at low and high magnification, and shows tests TN08 and TN07 (water, and brine respectively).
 258 The edges of the wear marks were selected for further analysis. Figures 6 shows detection of
 259 Cl in worn area of TN07 (brine), Figure 7 shows evidence of surface oxidation but no detection
 260 of Cl in worn area of TN08 (water), and Figure 8 shows, as expected no signals of Cl, as test
 261 was run in deionized water. In this case surface appears to be oxidized and is rich in Si (likely
 262 from ceramic Si₃N₄ ball).

263

264 The results shown in Figures 4-8 can be summarize as follows: (i) a solution of 50/50 wt%
 265 NaClO₄ to H₂O promotes wear when increasing the wear volume by over 45% in the
 266 tribological test; (ii) friction is significantly reduced by brine, compared with water; (iii)
 267 chlorine is detected in the wear track (<3 at%); and (iv) friction and wear data, combined with

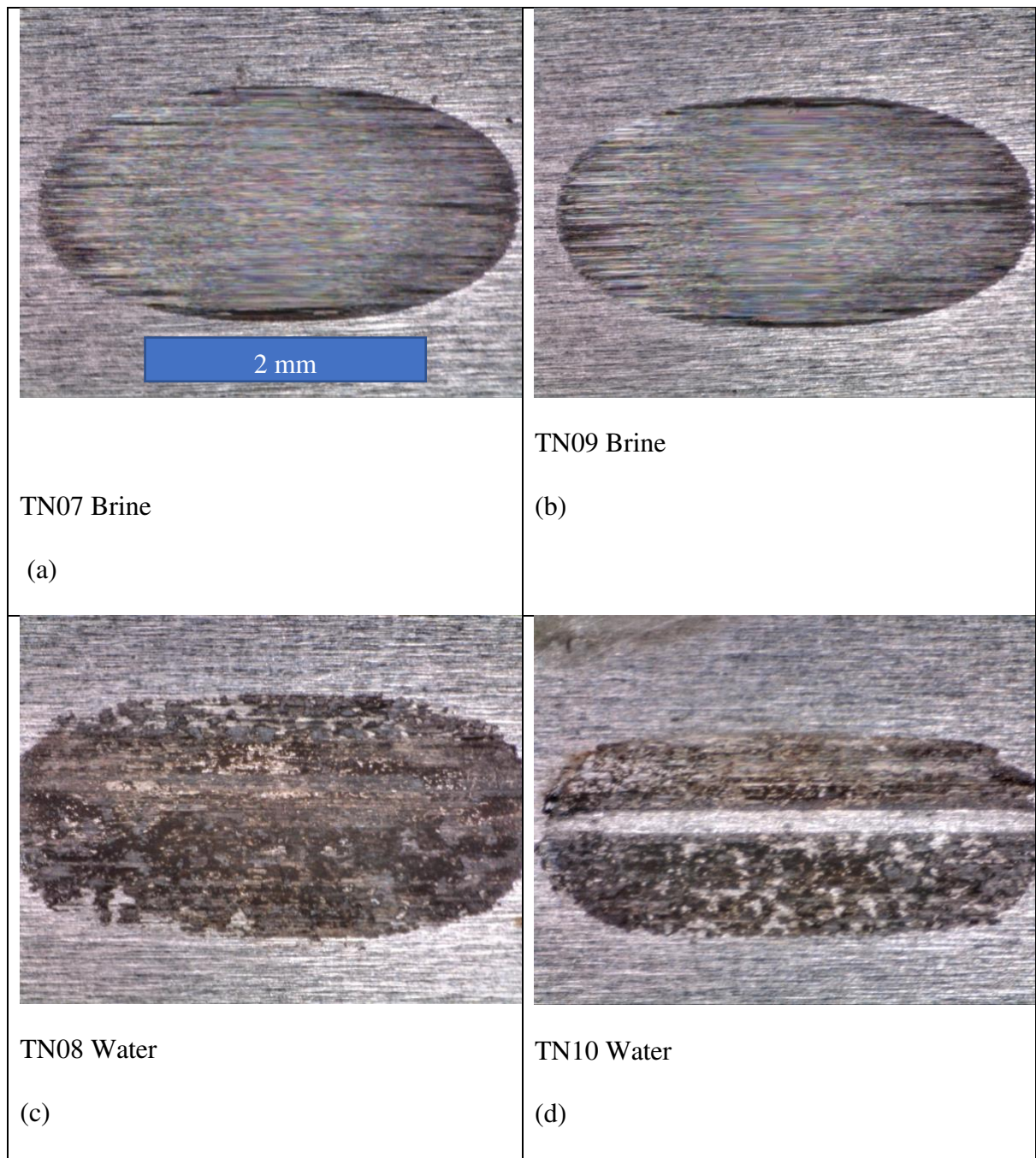
268 chemical analysis indicate that in comparison to water, the brine favors a sacrificial wear
269 mechanism, meaning that friction is reduced at the expense of higher wear.

270 The conclusion of these experiments is clear: brine accelerates wear by chemical reaction
271 leading to a sacrificial wear mechanism. Although the materials used in Mars exploration may
272 be resistant to chemical corrosion from brines in static conditions, mechanical wear only have
273 to remove a few nanometers of oxide to accelerate the corrosion. Tribocorrosion should not be
274 overlooked in selecting materials or special protective treatments for landed spacecraft and
275 structures that will support surface long-term operations for the human exploration of Mars,
276 and in particular for the wheels of the Martian rovers that will operate for long-term in the
277 harsh conditions of Mars.

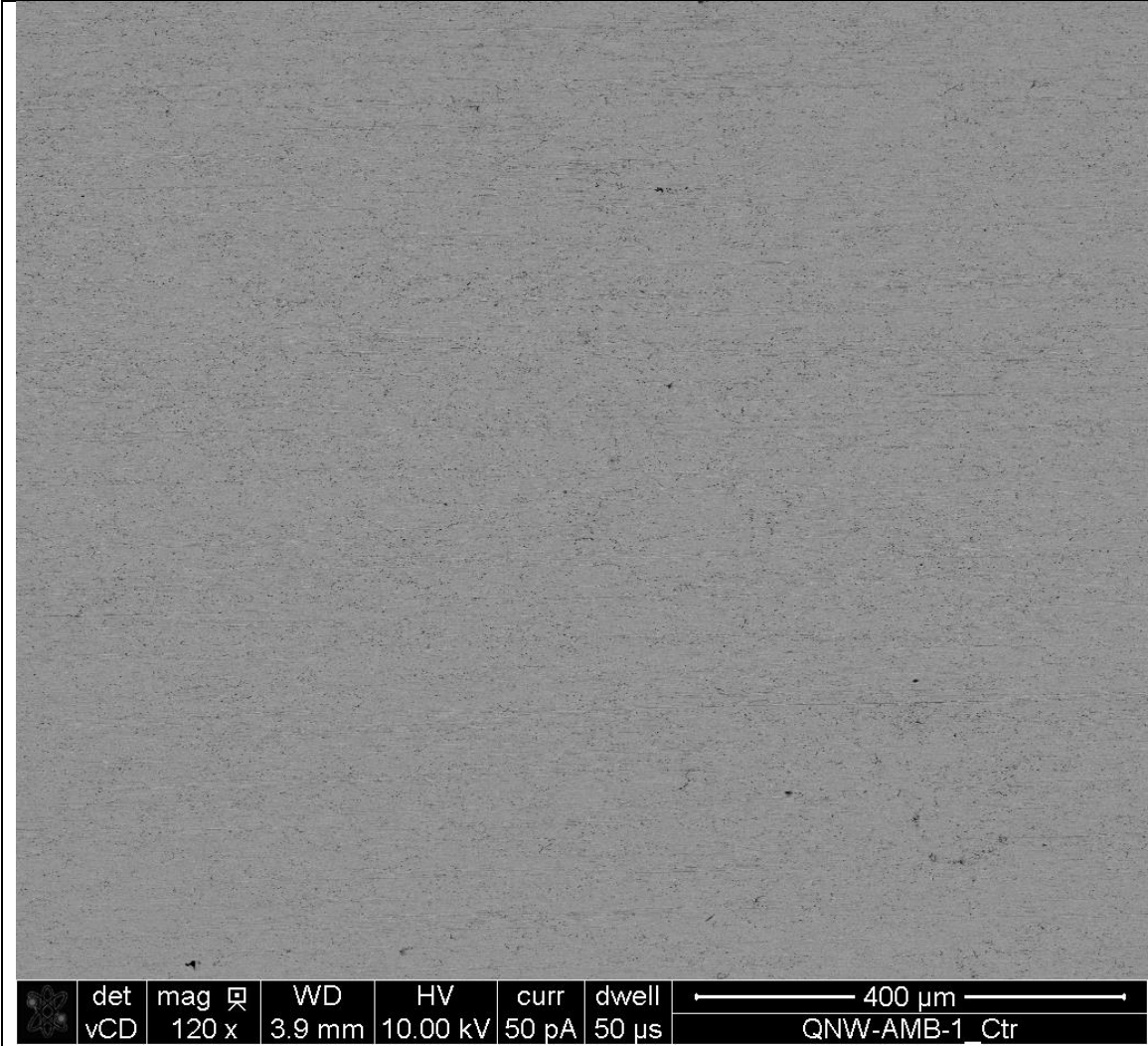
278 Further studies are needed to consider other important components of the Mars surface
279 environment that can affect this interaction such as: the effect of oxidants, the effect of radiation
280 on their oxidizing properties and the possible catalytic effects of the minerals present in the
281 Martian regolith, the diurnal thermal changes and variation in ambient humidity.

282

283



286 **Figure 4.** (a) Friction data (scale shown in Figure 2).



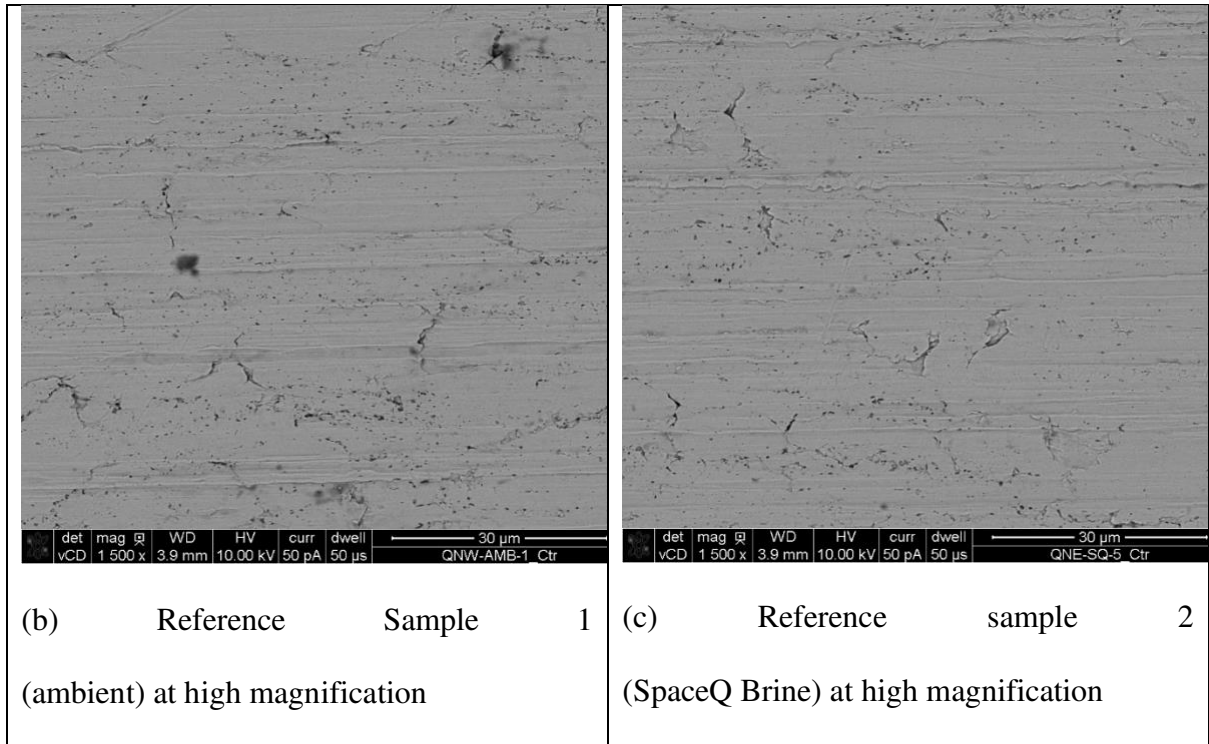
(a)

Reference

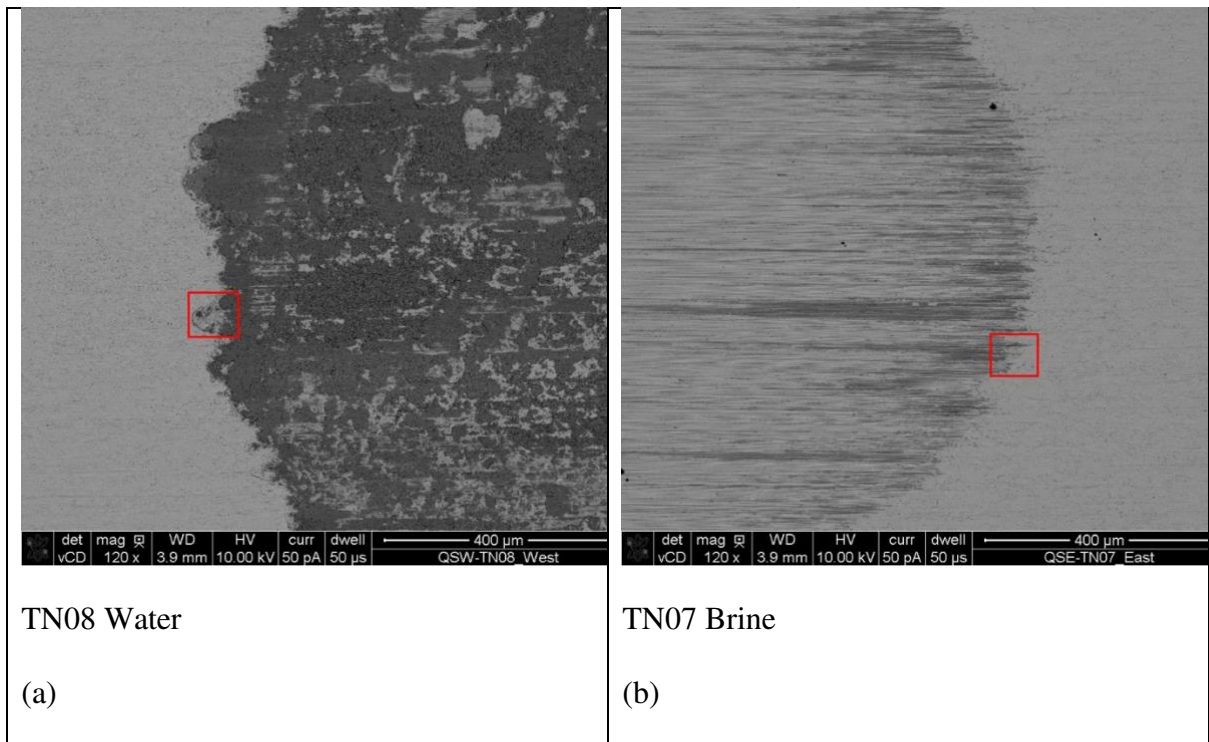
Sample

1

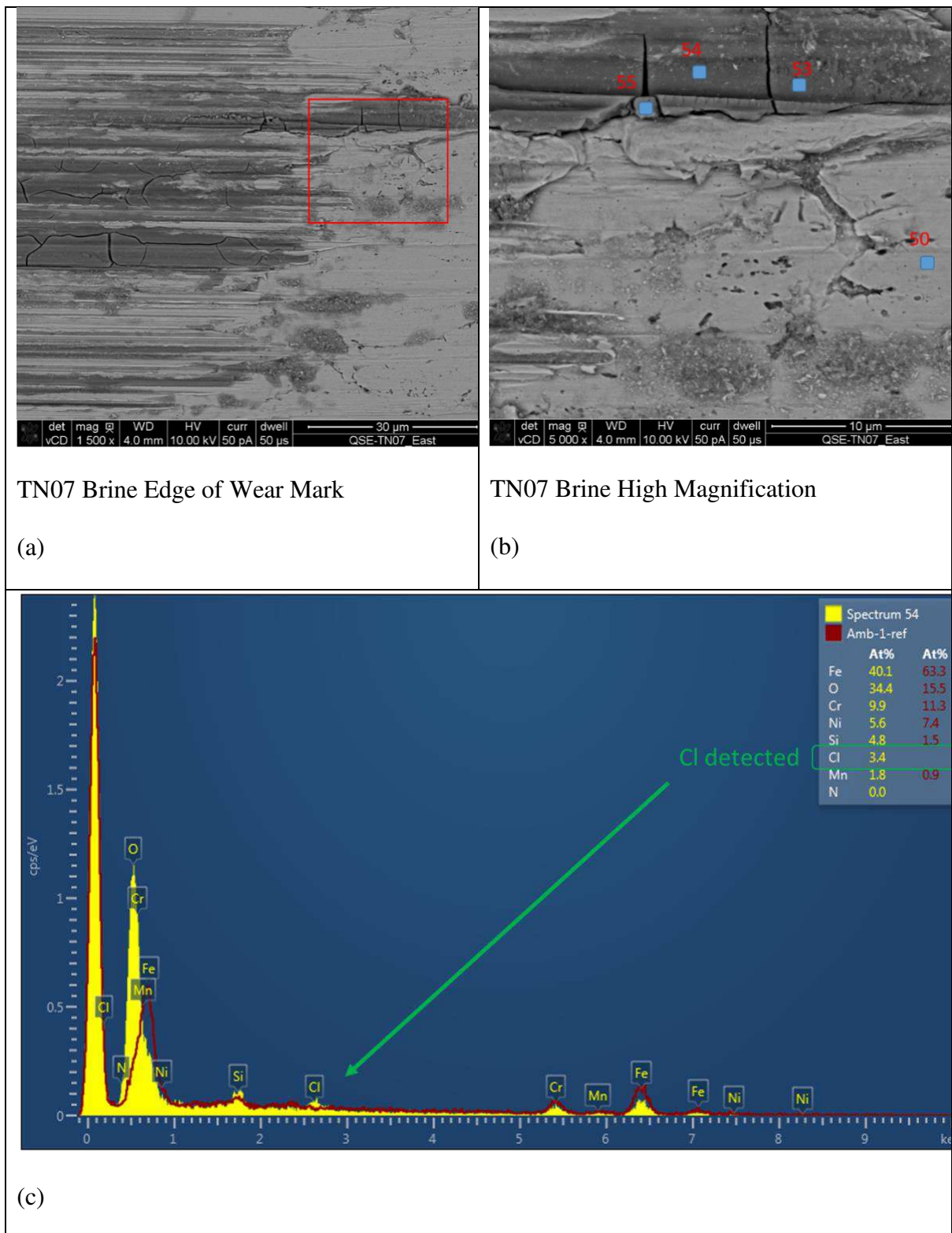
(ambient conditions) at low magnification



287 **Figure 5.** Reference samples (scale shown in the figures)



288 **Figure 6.** SEM overview of experiments (a) TN08 (water); and (b) TN07 (brine)



291 **Figure 7.** Detection of Cl in test with Brine.

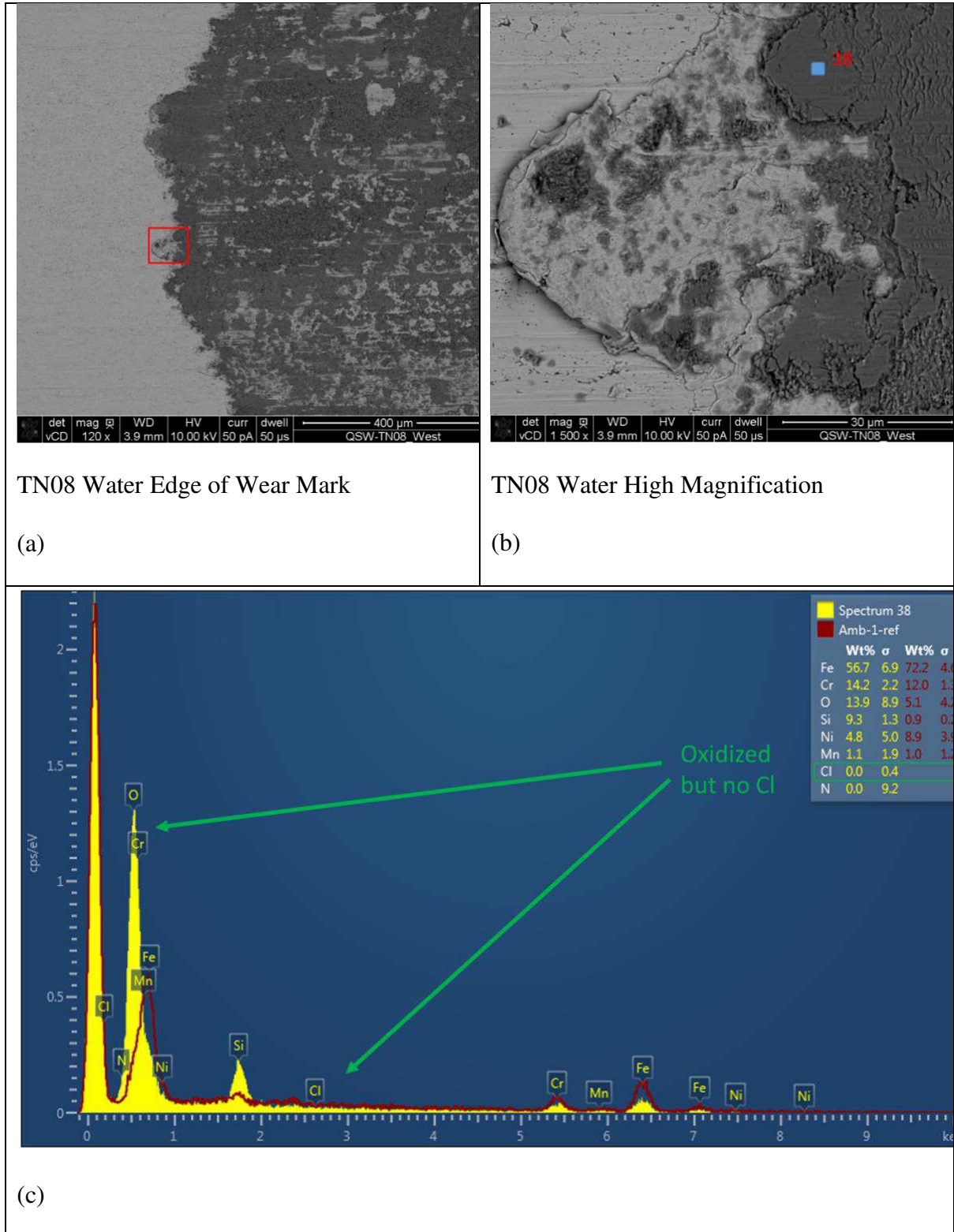
292

293

294

295

296



297 **Figure 8.** No Cl detected from water test.

298

299 **MATERIALS AND METHODS**

300

301 **The Effective Ground Pressure (EGP)**

302

303 Technical specifications of the Mars Exploration Rovers (Spirit and Opportunity) and Curiosity

304 wheels:

305

306 Curiosity (Mars Science Laboratory)

307 Mass = 960 kg

308 Rover Weight on Mars = 3572 N

309 Average Weight per Wheel = 595.3 N

310 Wheel Center Diameter = 0.500 m (with cleats)

311 Wheel Outer Diameter = 0.465 m (with cleats)

312 Wheel Width = 0.400 m

313

314 **Spirit and Opportunity**

315 Mass = 176.5 kg

316 Rover Weight on Mars = 656.7 N

317 Average Weight per Wheel = 109.45 N

318 Wheel Center Diameter = 0.262 m (with grouser bars)

319 Wheel Outer Diameter = 0.232 m (with grouser bars)

320 Wheel Width = 0.16 m

321

322 The cross-sectional area of each wheel's contact patch with the Ground Plane are 0.0173 m²

323 for Spirit and Opportunity; and 0.0901 m² for Curiosity.

324

325 The effective ground pressure (EGP) metric is defined as the average pressure under the
326 average wheel. The average weight on a wheel is first found by dividing the total vehicle
327 weight on a planetary body by the number of wheels. The EGP is found by dividing the average
328 weight by the cross sectional area of the wheel's contact patch on the ground plane, after the
329 wheel has sunk into a terrain so as to have a contact patch length of one wheel radius. In the
330 case of non-cylindrical tires, the largest radius, usually at the mid-plane is used.

331 When the wheel's periphery has cleats, lugs, or grouser bars; a determination is made as to the
332 amount of their height added to the tire diameter, based on the projected area ratio of these
333 tractive elements.

334

335 The EGP defined as the average weight over the CS Area are similar in the MER and Curiosity:

336

337 $EGP (\text{Opportunity}) = 109.45 \text{ N} / 0.0173 \text{ m}^2 = 6335 \text{ N/m}^2 = 6335 \text{ Pa} (0.919 \text{ psi})$

338

339 $EGP (\text{Curiosity}) = 595.3 \text{ N} / 0.0901 \text{ m}^2 = 6609 \text{ N/m}^2 = 6609 \text{ Pa} (0.959 \text{ psi})$

340

341 **Brine Corrosion tests**

342 The following steps were followed: (i) the chamber was first vacuumed and filled with pure
343 CO₂ gas till it reached 6 mbar; (ii) water was injected to create water vapor in the atmosphere;
344 (iii) the LN₂ was allowed to flow through the cooling plate which reached a temperature of 260
345 K and the temperature slowly increases due to the thermal equilibrium with the ambient lab
346 conditions; and (i) the experiment was stopped by opening the relief valve. The salt samples
347 deliquesced as the salt in it absorbed water from the atmosphere and formed brines.

348

349 **Simulation of martian near surface water cycle and thermal studies**

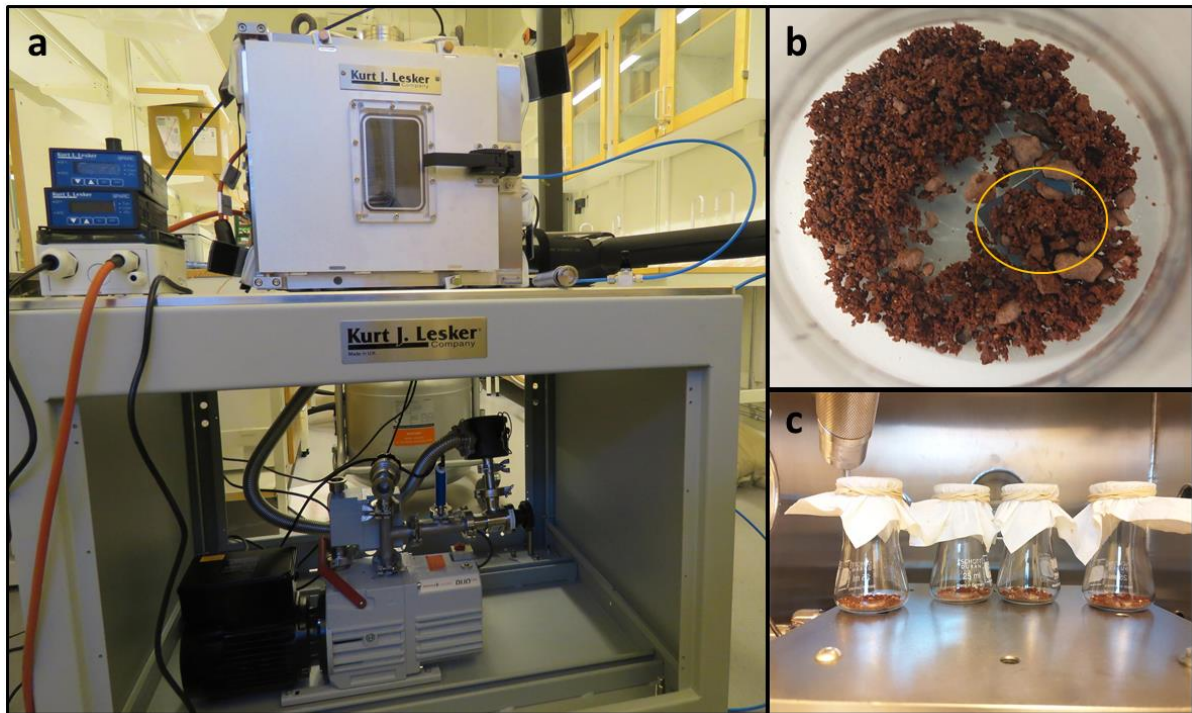
350

351 The experiments for brine corrosion under simulated Martian environment were conducted in the
352 SpaceQ chamber (figure 9), a cubical chamber with an internal volume of 27l. This chamber
353 can simulate temperatures ranging from 163 K to 423 K, pressures ranging from 10^{-5} mbar to
354 ambient conditions and relative humidity from 0% to 100%. Here we inject traces of water to
355 control the relative humidity using a stainless steel syringe connected to a ball valve in turn
356 connected to the chamber wall with the means of a swagelok connector. So, the water can be
357 injected several times during the experiment and as the ball valve opens the water is sucked
358 into the chamber and vaporises ²⁷.

359

360 We use sodium perchlorate salt (NaClO_4) (ACS reagent, $\geq 98.0\%$, 410241) bought from Sigma
361 Aldrich and the Mojave Martian Simulant (MMS-1) as Mars regolith simulant²⁹. We use the
362 “unsorted” grade bought from The Martian Garden-Austin Texas. The water used in the
363 injection is from Sigma which is filtered at $0.1\mu\text{m}$ to guarantee sterility and cleanliness (W4502).
364 We have conducted tests in SpaceQ Martian environment for two sets of samples prepared (i)
365 one with pure sodium perchlorate (NaClO_4) and one with a mixture of (ii) MMS + 10% NaClO_4
366 and exposed to Martian conditions. The samples were placed inside the SpaceQ and it was
367 simulated for the near surface water cycle condition as it will experience on Mars³⁰. The
368 chamber was first vacuumed and filled with pure CO_2 gas till it reached 6 mbar. Then, water
369 was injected to create water vapor in the atmosphere till RH reached 40% then the liquid
370 nitrogen (LN_2) is allowed to flow through the cooling plate which reached a temperature of
371 260 K and then temperature it let slowly to increase to ambient lab conditions due to the thermal
372 equilibrium. The experiment is stopped by opening the relief valve and the samples were
373 weighed (shown in Table 4). The samples with pure NaClO_4 were deliquesced and the samples

374 with mixture with the simulant were in a hydrated state as it absorbed water from the
375 atmosphere.



376
377 **Figure 9. Experimental setup** (a) Overview of the SpaceQ chamber (b) mixture of soil and
378 salt on a steel sample (c) samples placed on the cooling plate before experiment

379
380
381
382
383
384
385
386
387

Table 4: Summary of the weights for samples placed inside SpaceQ Martian environment

Weight (g)	Case 1	Case 2
------------	--------	--------

	(NaClO ₄ salt)			(MMS soil + 10% NaClO ₄ salt)		
	11R51	SS4301	S235	11R51	SS4301	S235
Initial	1.55 g	1.59 g	1.53 g	1.69 g	1.77 g	1.74 g
Final	2.32 g	2.33 g	2.37 g	1.83 g	2.04 g	1.89 g
Increase in weight	0.77 g	0.74 g	0.84 g	0.14 g	0.27 g	0.15 g

388

389

390 **Tribocorrosion tests**

391

392 The following materials were used:

- 393 • **Material 1:** Stainless steel (Sandvik 11R51)
- 394 • **Material 2:** Ceramic bearing ball (Si₃N₄), 10 mm diameter.
- 395 • **Fluid medium:**
 - 396 ○ “Brine” (50/50 wt% solution of NaClO₄+H₂O).
 - 397 ○ “Water” (deionized water, H₂O)

398 The following methods have been used

- 399 • **Tribological experiment:** Optimol SRV, normally used for material development,
400 (screening of surface-lubricant combinations)
 - 401 ○ Applied Load 25 N. Contact pressure ~1 GPa.
 - 402 ■ Selected based on reasonable assumption: Few kg load onto “pointy but not sharp”-
403 rock...
 - 404 ○ Ambient temperature, Atmosphere: N₂ > 95%, remaining is O₂
 - 405 ○ Wear test for 54 000 cycles (2 mm reciprocal, = 216 m sliding distance)

406 • **Surface analysis**

407 ○ A Zygo NewView 7300 **3D optical profilometer** (Zygo Corporation, Middlefield, CT,
408 USA) was employed for surface topography analysis. Measurements were conducted under
409 both 10x magnification. The surface profilometry data was analysed using MountainsMap
410 Premium 7.4 (Digital Surf, France).

411 Scanning Electron Microscopy (**SEM**) and Electron Dispersive X-ray Spectroscopy (**EDS**)
412 was employed for high magnification surface analysis including chemical (elemental) analysis:
413 Magellan 400 FEG-SEM (FEI Company, Eindhoven, The Netherlands). EDS was performed
414 using an X-Max 80 mm² X-ray detector (Oxford Instruments, Abingdon, UK) operated at 10
415 kV and 50 pA.

416

417

418

420 **References**

421

- 422 1 Watson, S. W., Friedersdorf, F. J., Madsen, B. W. & Cramer, S. D. Methods of
423 measuring wear-corrosion synergism. *Wear* **181-183**, 476-484, doi:10.1016/0043-
424 1648(95)90161-2 (1995).
- 425 2 Edison, T. Improvement in Telegraph Apparatus. (1875).
- 426 3 International Organization for, S. *Corrosion of metals and alloys – Vocabulary (ISO*
427 *8044:2020)*. (2020).
- 428 4 American Society for, T. & Materials. (2017).
- 429 5 Landolt, D. & Mischler, S. *Tribocorrosion of Passive Metals and Coatings*.
430 (Woodhead Publishing Limited, 2011).
- 431 6 Rowe, G. W. The chemistry of tribology, friction, lubrication and wear. *Royal Institute*
432 *of Chemistry, Reviews* **1**, 135-204, doi:10.1039/RR9680100135 (1968).
- 433 7 Bhardwaj, A., Sam, L., Martín-Torres, F. J. & Zorzano, M. P. Are Slope Streaks
434 Indicative of Global-Scale Aqueous Processes on Contemporary Mars? *Reviews of*
435 *Geophysics* **57**, 48-77, doi:10.1029/2018rg000617 (2019).
- 436 8 Bhardwaj, A., Sam, L., Martín-Torres, F. J., Zorzano, M. P. & Fonseca, R. M. Martian
437 slope streaks as plausible indicators of transient water activity. *Sci Rep* **7**, 7074,
438 doi:10.1038/s41598-017-07453-9 (2017).
- 439 9 Clark, B., and van Hart, D. The salts of Mars. *Icarus* **45**, 370-378 (1981).
- 440 10 Hecht, M. H. *et al.* Detection of perchlorate and the soluble chemistry of martian soil
441 at the Phoenix lander site. *Science* **325**, 64-67, doi:10.1126/science.1172466 (2009).
- 442 11 Navarro-González, R., Vargas, E., de la Rosa, J., Raga, A. C. & McKay, C. P.
443 Reanalysis of the Viking results suggests perchlorate and organics at midlatitudes on
444 Mars. *Journal of Geophysical Research* **115**, doi:10.1029/2010je003599 (2010).
- 445 12 Glavin, D. P. *et al.* Evidence for perchlorates and the origin of chlorinated hydrocarbons
446 detected by SAM at the Rocknest aeolian deposit in Gale Crater. *Journal of*
447 *Geophysical Research: Planets* **118**, 1955-1973, doi:10.1002/jgre.20144 (2013).
- 448 13 Kounaves, S. P., Carrier, B. L., O’Neil, G. D., Stroble, S. T. & Claire, M. W. Evidence
449 of martian perchlorate, chlorate, and nitrate in Mars meteorite EETA79001:
450 Implications for oxidants and organics. *Icarus* **229**, 206-213,
451 doi:10.1016/j.icarus.2013.11.012 (2014).
- 452 14 Catling, D. C. *et al.* Atmospheric origins of perchlorate on Mars and in the Atacama.
453 *Journal of Geophysical Research* **115**, doi:10.1029/2009je003425 (2010).
- 454 15 Tennakone, K. Contact Electrification of Regolith Particles and Chloride Electrolysis:
455 Synthesis of Perchlorates on Mars. *Astrobiology* **16**, 811-816,
456 doi:10.1089/ast.2015.1424 (2016).
- 457 16 Carrier, B. L. & Kounaves, S. P. The origins of perchlorate in the Martian soil.
458 *Geophysical Research Letters* **42**, 3739-3745, doi:10.1002/2015gl064290 (2015).
- 459 17 Ojha, L. *et al.* Spectral evidence for hydrated salts in recurring slope lineae on Mars.
460 *Nature Geoscience* **8**, 829-832, doi:10.1038/ngeo2546 (2015).
- 461 18 Martín-Torres, F. J. *et al.* Transient liquid water and water activity at Gale crater on
462 Mars. *Nature Geoscience* **8**, 357-361, doi:10.1038/ngeo2412 (2015).
- 463 19 Rivera-Valentín, E. G., Chevrier, V. F., Soto, A. & Martínez, G. Distribution and
464 habitability of (meta)stable brines on present-day Mars. *Nature Astronomy*,
465 doi:10.1038/s41550-020-1080-9 (2020).

- 466 20 Osterloo, M. M., Anderson, F. S., Hamilton, V. E. & Hynek, B. M. Geologic context
467 of proposed chloride-bearing materials on Mars. *Journal of Geophysical Research* **115**,
468 doi:10.1029/2010je003613 (2010).
- 469 21 Chevrier, V. F. & Altheide, T. S. Low temperature aqueous ferric sulfate solutions on
470 the surface of Mars. *Geophysical Research Letters* **35**, doi:10.1029/2008gl035489
471 (2008).
- 472 22 Schroder, C. *et al.* Amazonian chemical weathering rate derived from stony meteorite
473 finds at Meridiani Planum on Mars. *Nat Commun* **7**, 13459, doi:10.1038/ncomms13459
474 (2016).
- 475 23 Calle, L. M. Corrosion on Mars: Effect of the Mars Environment on Spacecraft
476 Materials. (2019).
- 477 24 Vargel, C. Corrosium of aluminium. 700 pp (2004).
- 478 25 Calle, L. M., W. Li, M. R. Johansen, J. W. Buhrow, and C. I. Calle. Corrosion on Mars:
479 An Investigation under Relevant Simulated Martian Environments. (2017).
- 480 26 Vago, J. L. *et al.* Habitability on Early Mars and the Search for Biosignatures with the
481 ExoMars Rover. *Astrobiology* **17**, 471-510, doi:10.1089/ast.2016.1533 (2017).
- 482 27 Vakkada Ramachandran, A., Nazariou, M I, Mathanlal, T, Zorzano, M-P, Martin-
483 Torres, J Space environmental chamber for planetary studies. *Sensors* **under review**
484 (2020).
- 485 28 Rudnick, L. R. Lubricant additives : chemistry and application. (2003).
- 486 29 Peters, G. H. *et al.* Mojave Mars simulant—Characterization of a new geologic Mars
487 analog. *Icarus* **197**, 470-479, doi:10.1016/j.icarus.2008.05.004 (2008).
- 488 30 Martin-Torres, J. *et al.* The HABIT (HabitAbility: Brine Irradiation and Temperature)
489 environmental instrument for the ExoMars 2022 Surface Platform. *Planetary and*
490 *Space Science*, 104968, doi:<https://doi.org/10.1016/j.pss.2020.104968> (2020).
- 491

492

493 **Acknowledgements**

494 M-P. Z's contribution has been partially supported by the Spanish State Research Agency
495 (AEI) Project No. MDM-2017-0737 Unidad de Excelencia "María de Maeztu" - Centro de
496 Astrobiología (CSIC-INTA). We thank the ExoMars project team, European Space Agency
497 (ESA), for the review of the manuscript. The SpaceQ chamber has been developed together
498 with Kurt J. Lesker Company and was funded by the Kempe Foundation.

499

500 **Author contributions.** JMT: Conceptualization, Supervision, Investigation, writing original
501 draft, funding acquisition, resources; MPZ: Conceptualization, methodology, supervision,
502 investigation, writing original draft, funding acquisition; EN: Tribocorrosion and corrosion
503 experiments, writing, review & editing; AVR: Corrosion experiments, and experimental

504 support to tribocorrosion experiments, writing, review & editing; AB: Writing, review &
505 editing.

506 **Declaration of competing interest**

507 The authors declare that they have no known competing financial interests or personal
508 relationships that could have appeared to influence the work reported in this paper.

509

510

Figures

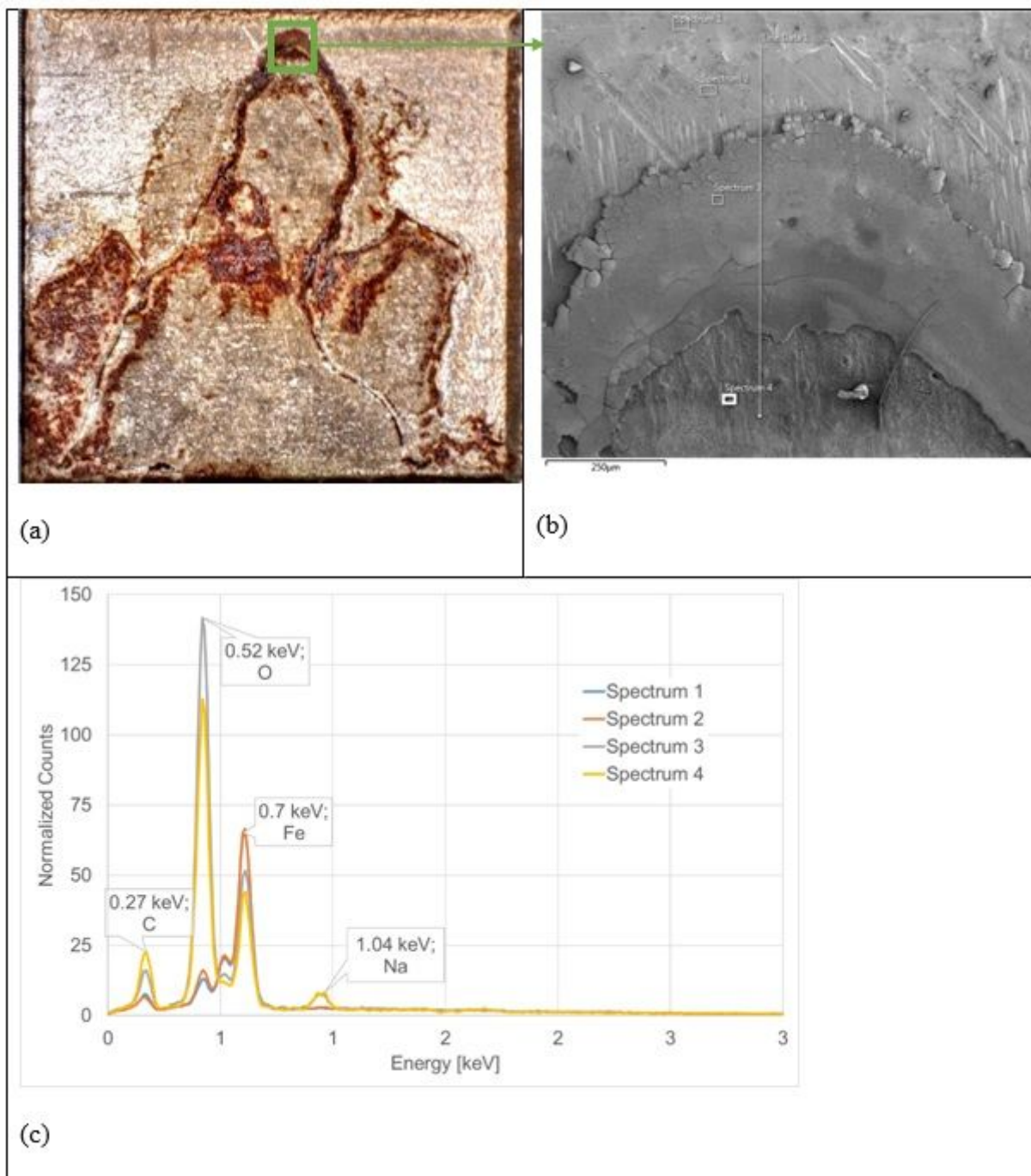


Figure 1

(a) Microscope image of 10x10 mm Regular Steel sample. (b) High magnification SEM image showing location of EDS analyzed regions. (c) results of EDS analysis confirming corrosion by detection of Na and O in Spectrum 3 and 4.



Figure 2

Setup of tribological experiment showing ceramic ball and stainless-steel plate in their respective sample holders.

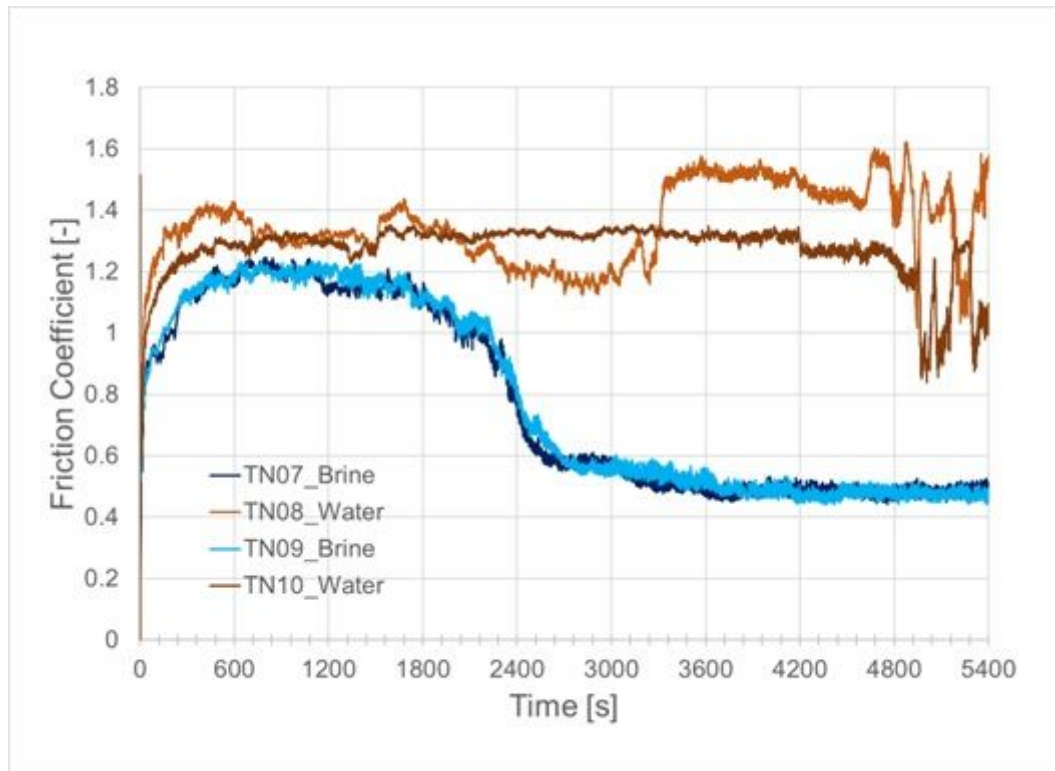


Figure 3

Friction data indicates transition to corrosive wear around Time=1800 s when immersed in brine.

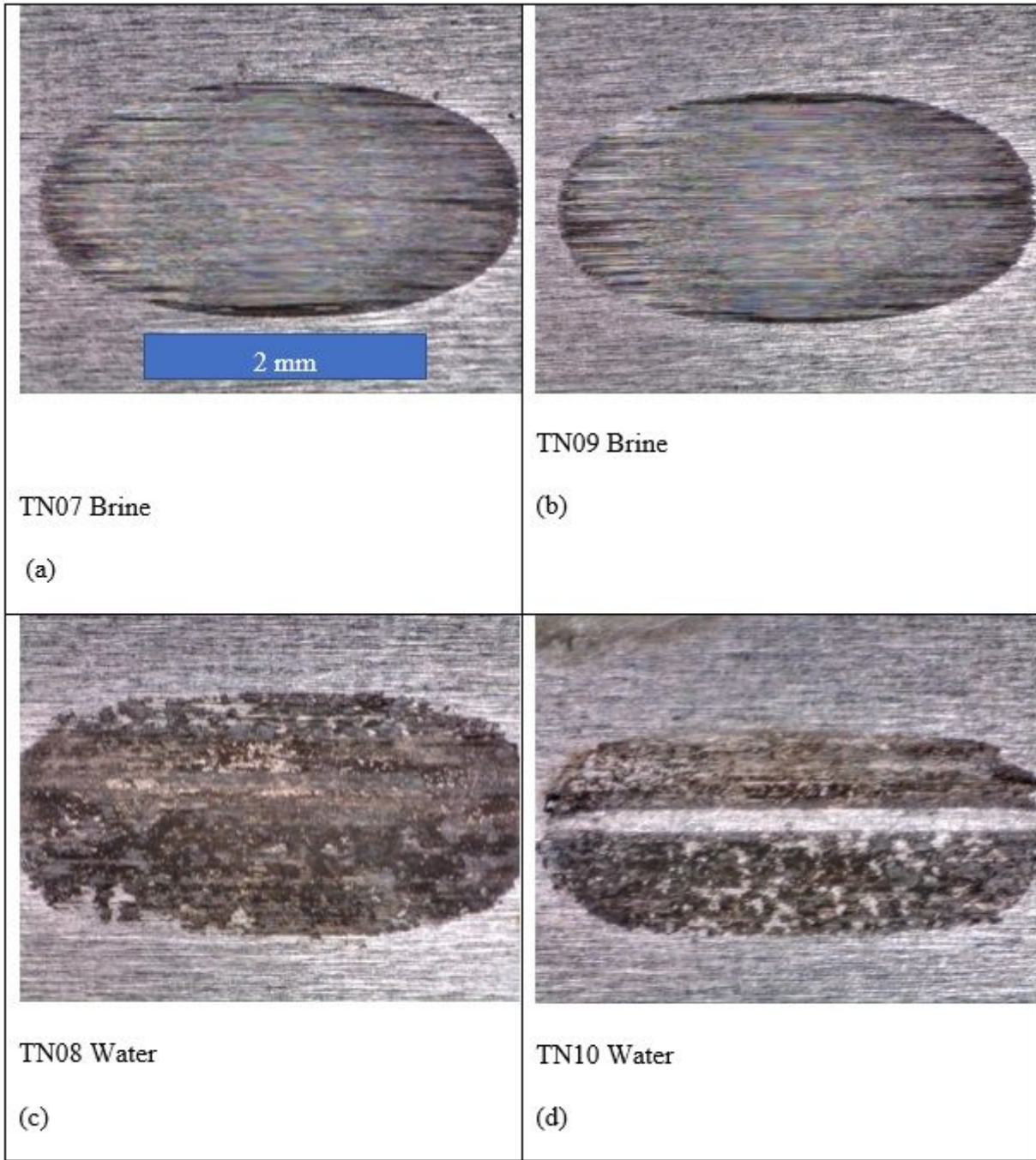


Figure 4

(a) Friction data (scale shown in Figure 2).

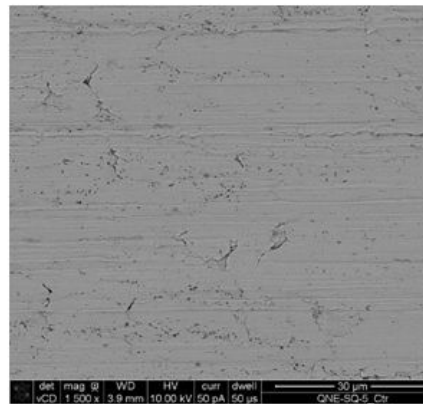
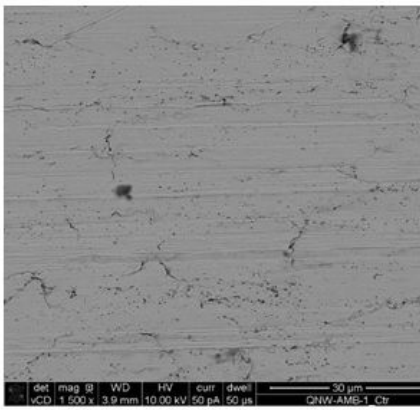
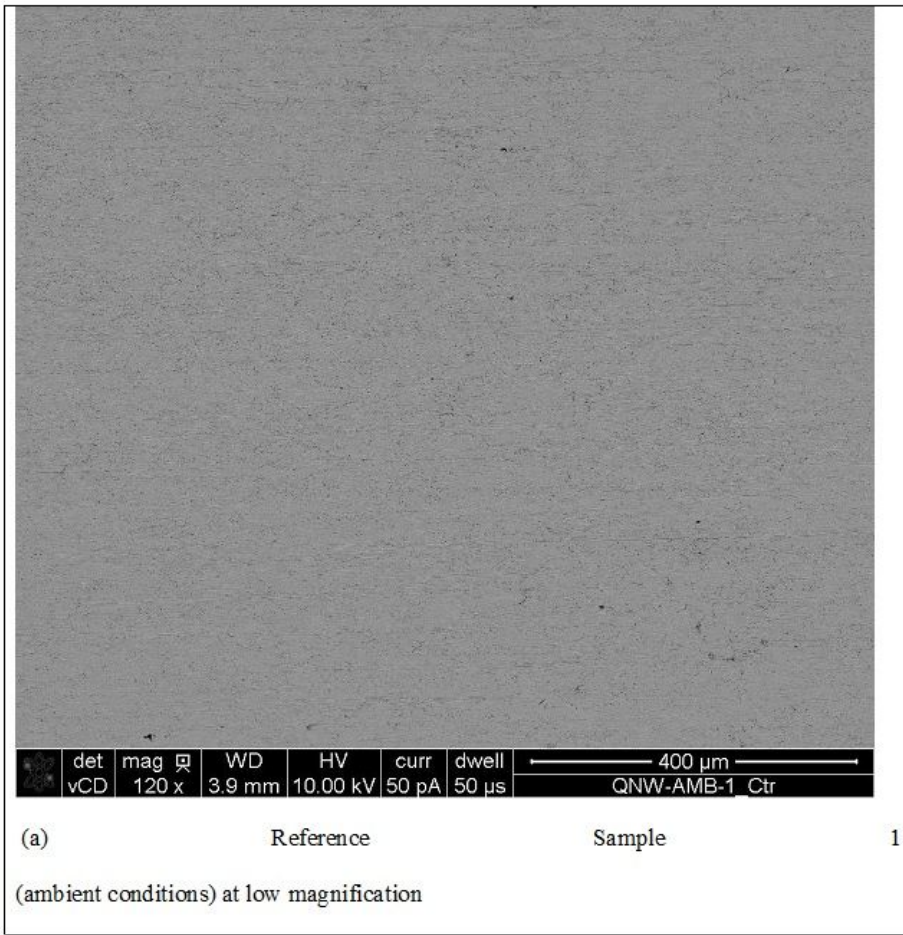


Figure 5

Reference samples (scale shown in the figures)

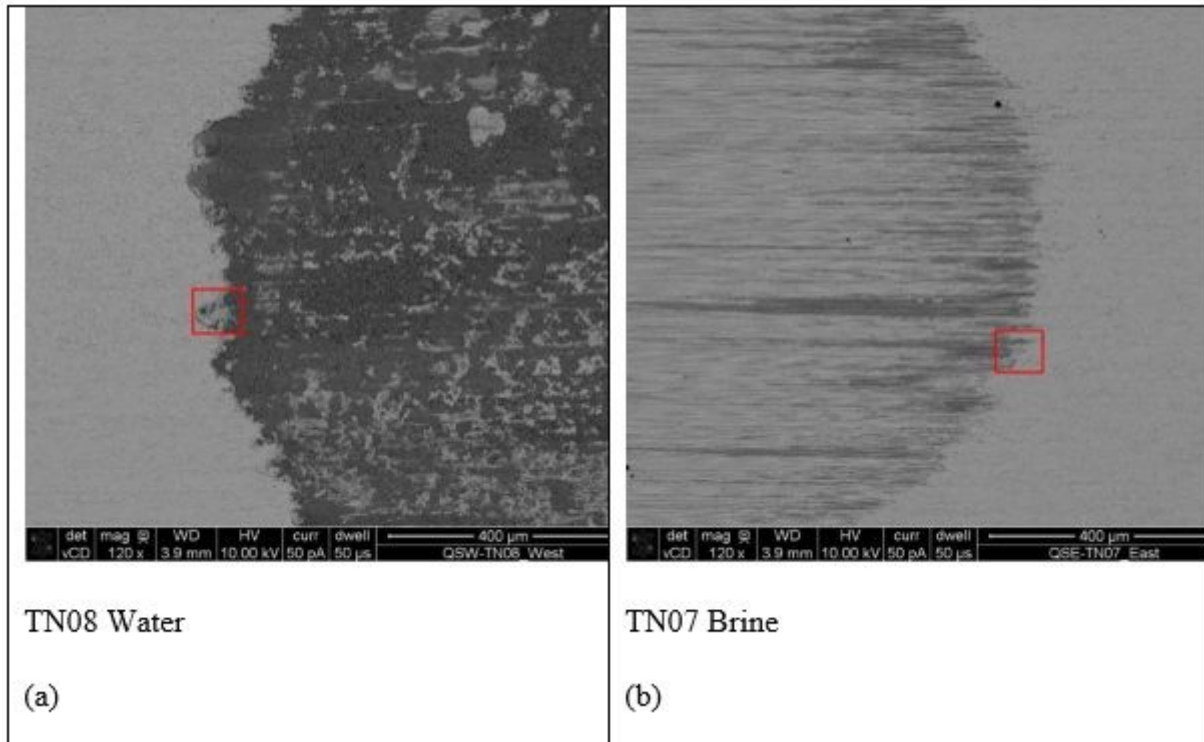


Figure 6

SEM overview of experiments (a) TN08 (water); and (b) TN07 (brine)

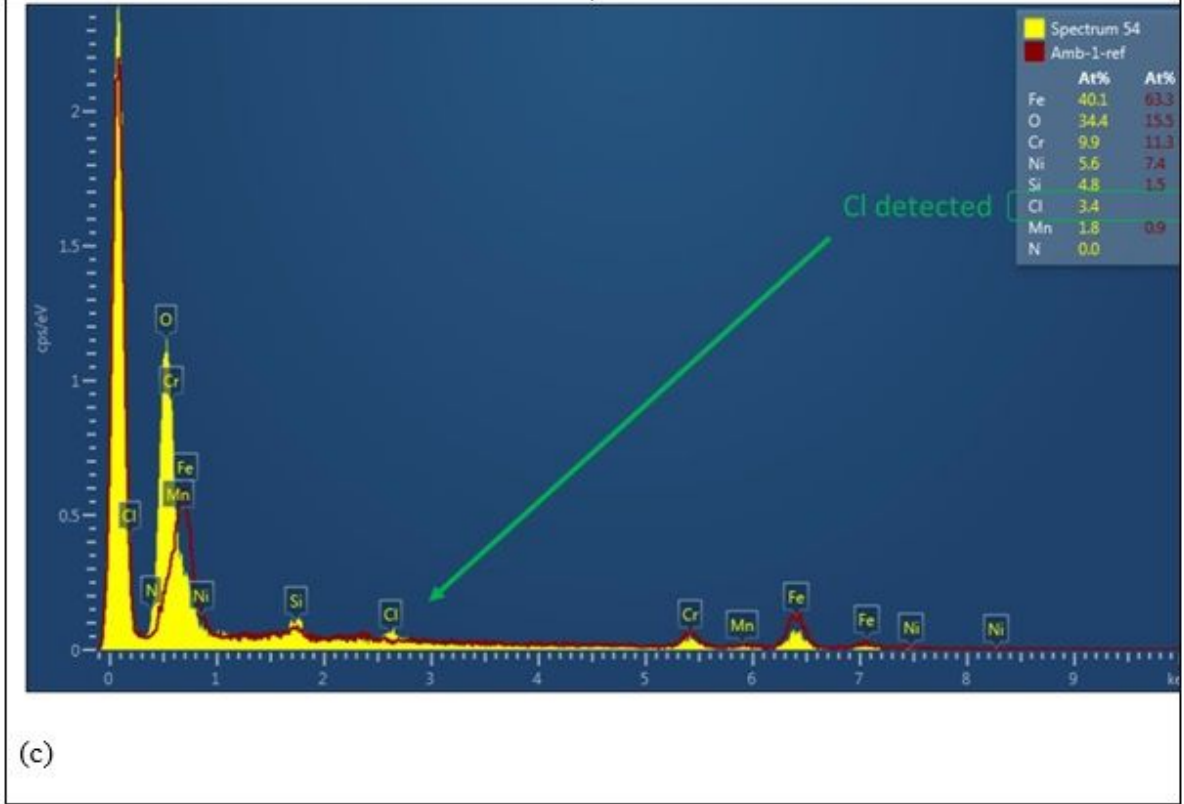
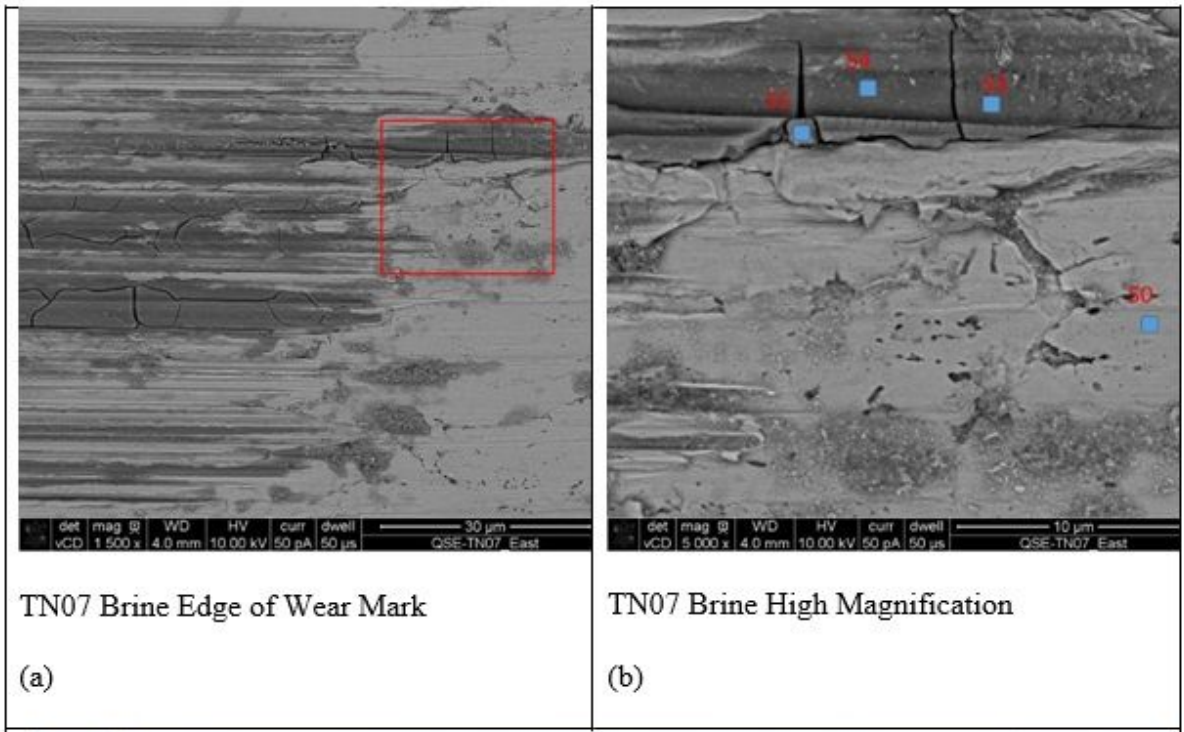


Figure 7
 Detection of Cl in test with Brine.

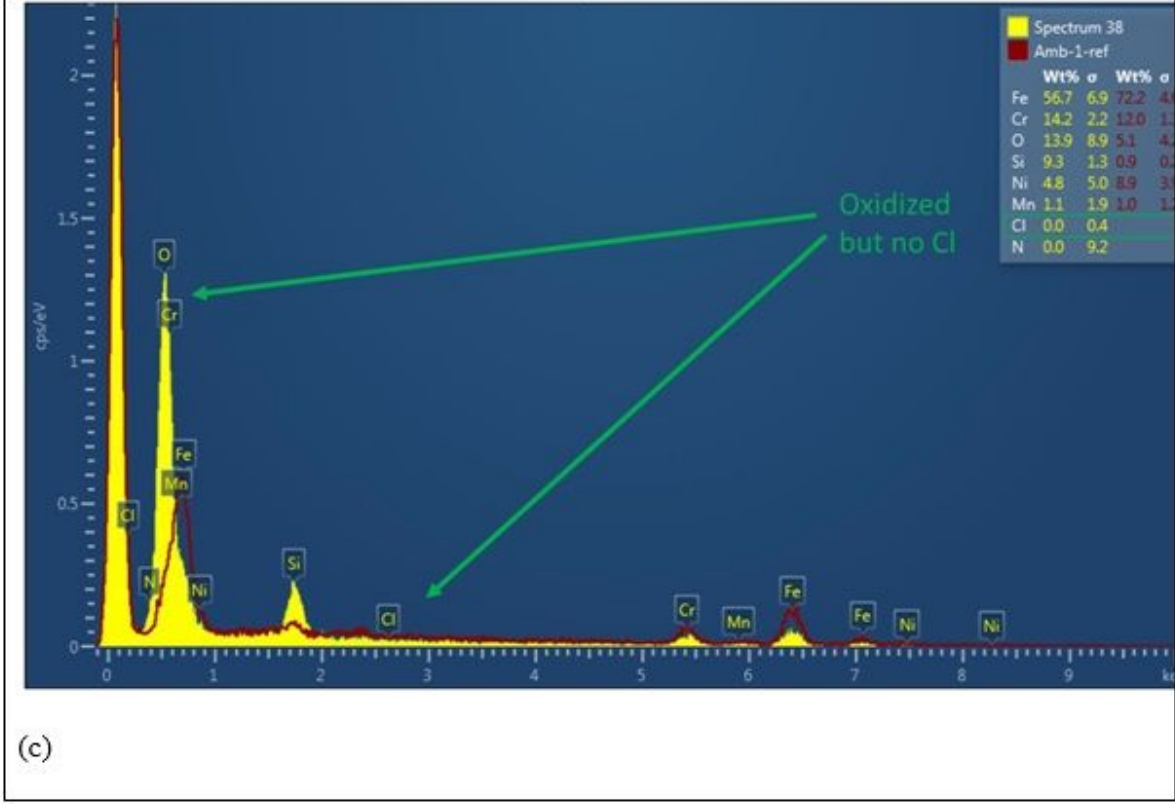
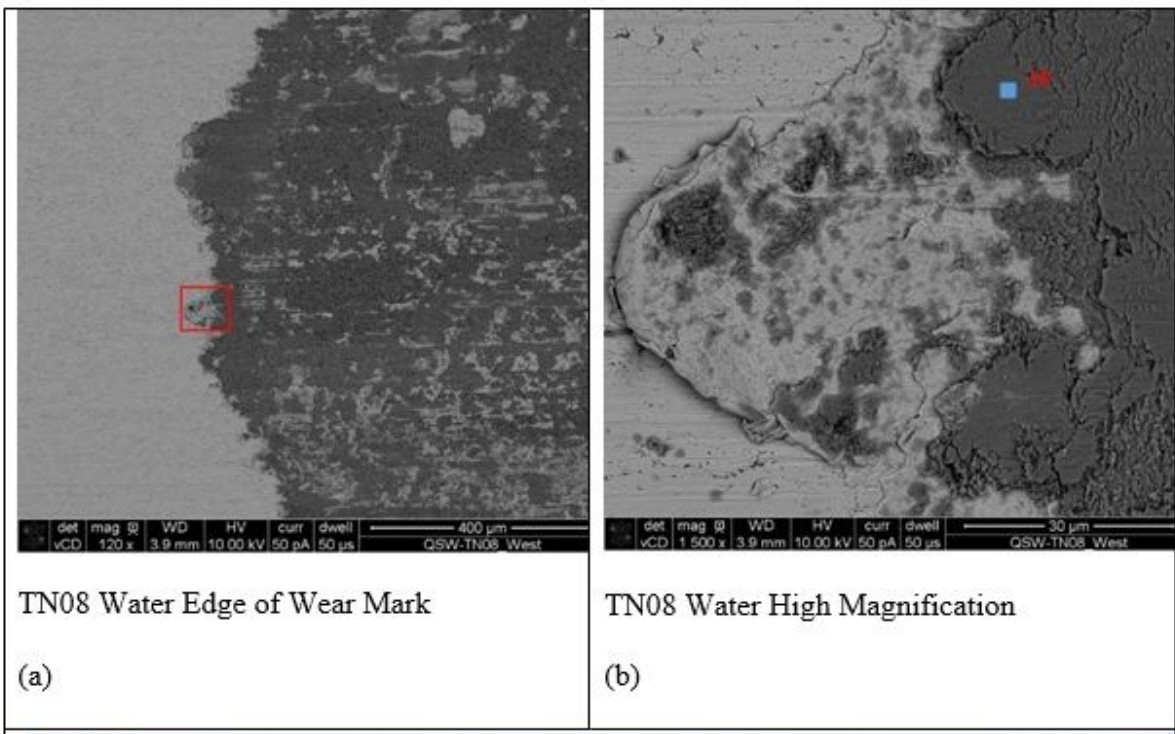


Figure 8

No Cl detected from water test.

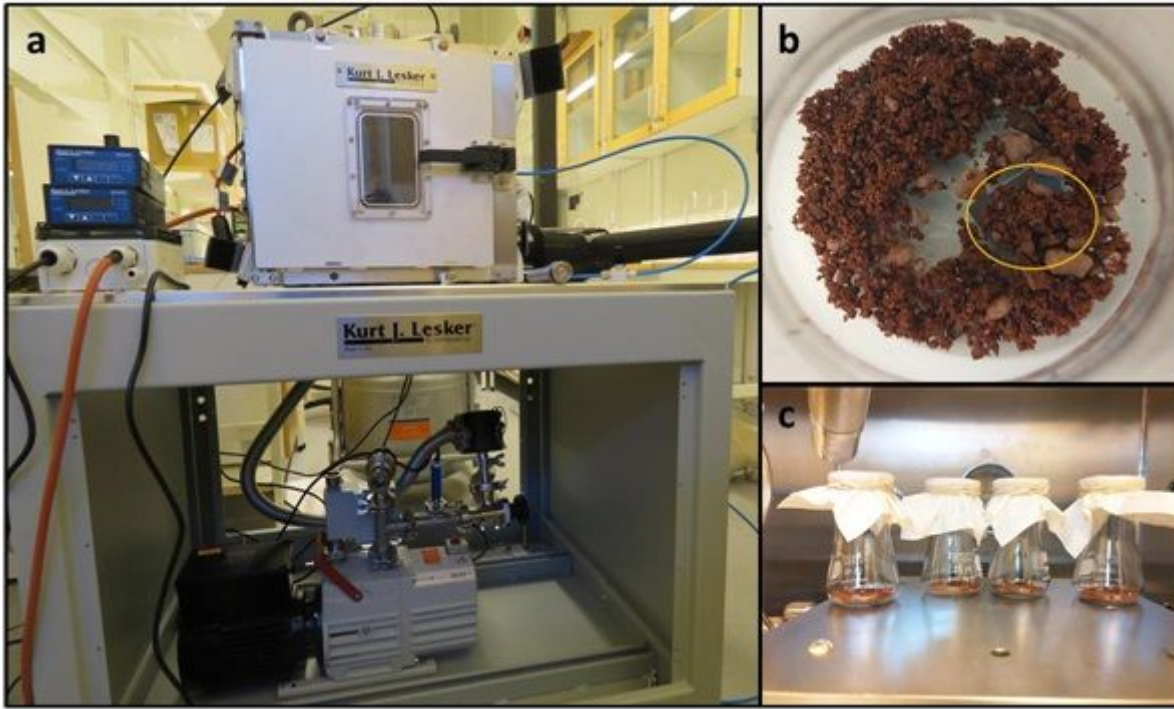


Figure 9

Experimental setup (a) Overview of the SpaceQ chamber (b) mixture of soil and salt on a steel sample (c) samples placed on the cooling plate before experiment